LUND UNIVERSITY

Impact of doping and diameter on the electrical properties of GaSb nanowires

Babadi, Aein S.; Svensson, Johannes; Lind, Erik; Wernersson, Lars Erik

Published in:
Applied Physics Letters

DOI:
10.1063/1.4975374

2017

Link to publication

Citation for published version (APA):
Babadi, A. S., Svensson, J., Lind, E., & Wernersson, L. E. (2017). Impact of doping and diameter on the electrical properties of GaSb nanowires. *Applied Physics Letters*, *110*(5), Article 053502. https://doi.org/10.1063/1.4975374

Total number of authors:
4

General rights
Unless other specific re-use rights are stated the following general rights apply:
Copyright and moral rights for the publications made accessible in the public portal are retained by the authors and/or other copyright owners and it is a condition of accessing publications that users recognise and abide by the legal requirements associated with these rights.
• Users may download and print one copy of any publication from the public portal for the purpose of private study or research.
• You may not further distribute the material or use it for any profit-making activity or commercial gain
• You may freely distribute the URL identifying the publication in the public portal

Read more about Creative commons licenses: https://creativecommons.org/licenses/

Take down policy
If you believe that this document breaches copyright please contact us providing details, and we will remove access to the work immediately and investigate your claim.

LUND UNIVERSITY

PO Box 117
221 00 Lund
+46 46-222 00 00

Download date: 17. May. 2025

Impact of doping and diameter on the electrical properties of GaSb nanowires

Aein S. Babadi, Johannes Svensson, Erik Lind, and Lars-Erik Wernersson

Citation: Appl. Phys. Lett. **110**, 053502 (2017); doi: 10.1063/1.4975374
View online: http://dx.doi.org/10.1063/1.4975374
View Table of Contents: http://aip.scitation.org/toc/apl/110/5
Published by the American Institute of Physics

Articles you may be interested in

Electronic structure and electron mobility in Si1– xGex nanowires
Appl. Phys. Lett. **110**, 052102052102 (2017); 10.1063/1.4975066

Nontrivial surface state transport in Bi2Se3 topological insulator nanoribbons
Appl. Phys. Lett. **110**, 053108053108 (2017); 10.1063/1.4975386

Chemical vapor deposition of monolayer MoS2 directly on ultrathin Al2O3 for low-power electronics
Appl. Phys. Lett. **110**, 053101053101 (2017); 10.1063/1.4975064

Strong coupling between Tamm plasmon polariton and two dimensional semiconductor excitons
Appl. Phys. Lett. **110**, 051101051101 (2017); 10.1063/1.4974901

Photoconduction properties and anomalous power-dependent quantum efficiency in non-polar ZnO epitaxial films grown by chemical vapor deposition
Appl. Phys. Lett. **110**, 052101052101 (2017); 10.1063/1.4974924

Improved integration of ultra-thin high-k dielectrics in few-layer MoS2 FET by remote forming gas plasma pretreatment
Appl. Phys. Lett. **110**, 053110053110 (2017); 10.1063/1.4975627

Fearful for the future of science?
Sign up for FREE FYI emails.
AIP | American Institute of Physics

APPLIED PHYSICS LETTERS **110**, 053502 (2017)

Impact of doping and diameter on the electrical properties of GaSb nanowires

Aein S. Babadi,[a] Johannes Svensson, Erik Lind, and Lars-Erik Wernersson
Department of Electrical and Information Technology, Lund University, Lund SE-22100, Sweden

(Received 10 November 2016; accepted 20 January 2017; published online 2 February 2017)

The effect of doping and diameter on the electrical properties of vapor-liquid-solid grown GaSb nanowires was characterized using long channel back-gated lateral transistors and top-gated devices. The measurements showed that increasing the doping concentration significantly increases the conductivity while reducing the control over the channel potential and shifting the threshold voltage, as expected. The highest average mobility was 85 cm^2/V·s measured for an unintentionally doped GaSb nanowire with a diameter of 45 nm, whereas medium doped nanowires with large diameters (81 nm) showed a value of 153 cm^2/V·s. The mobility is found to be independent of nanowire diameter in the range of 36 nm–68 nm, while the resistivity is strongly reduced with increasing diameter attributed to the surface depletion of charge carriers. The data are in good agreement with an analytical calculation of the depletion depth. A high transconductance was achieved by scaling down the channel length to 200 nm, reaching a maximum value of 80 μS/μm for a top-gated GaSb nanowires transistor with an ON-resistance of 26 kΩ corresponding to 3.9 Ω.mm. The lowest contact resistance obtained was 0.35 Ω·mm for transistors with the highest doping concentration. *Published by AIP Publishing*. [http://dx.doi.org/10.1063/1.4975374]

Semiconductor nanowires (NWs) are promising building blocks for the next-generation nanoscale electronics due to their good electrostatics enabling aggressive gate length scaling.[1–3] The nanoscale geometry of NWs may provide strain accommodation through radial relaxation enabling high lattice-mismatch heteroepitaxy on, e.g., Si substrates with high crystal quality.[4] While the synthesis, processing, and applications of III–V materials have been studied for more than a decade, research on III-Sb NWs has attracted a growing interest only recently.[5–9] GaSb, in particular, is an increasingly important material for a III–V p-channel metal-oxide-semiconductor field-effect transistor (MOSFET) due to its high hole mobility.[10] However, the mobility is highly dependent on the materials synthesis method and device structure. It is therefore important to further study the impact of, e.g., geometry and doping on the transport properties.

Diameter-dependent charge transport has been used to characterize the impact of surface scattering on the carrier mobility for both n- and p-type nanowires. The most common observed trend is a decrease in mobility due to the stronger influence of surface scattering for smaller diameters.[11,12] However, there have also been reports that the diameter has no impact on the mobility for InAs n-type NWs with a diameter >40 nm.[13] Apart from the diameter, doping control, which allows for determining the threshold voltage and reducing access resistances, is also crucial. The few efforts devoted to charge transport in GaSb nanowires[14] suggest a necessity for additional detailed and systematic studies. In this work, we present a comparative study of the influence of p-doping by (Zn) and nanowire diameter on the transport properties of GaSb nanowires focusing on nanowires with the diameters of about 30–70 nm.

InAs/GaSb nanowires were grown using the vapor-liquid-solid mechanism in the MOVPE system. Nanowires were grown from Au seed particles with a thickness of 15 nm and diameters of 24–32 nm patterned on the substrate consisted of an InAs epitaxial layer on Si(111)[15] by electron beam lithography (EBL). The use of EBL enables accurate control of the Au particle diameter and pitch, which is crucial for obtaining uniform nanowire length and diameter. After annealing in arsine at 500 °C, an InAs stem was grown for 10 min at 420 °C using trimethylindium (TMIn) and arsine with molar fractions of $X_{TMIn} = 2.8 \times 10^{-6}$ and $X_{Arsine} = 1.9 \times 10^{-4}$, respectively. This is followed by an at least 1 μm long GaSb segment grown for 35 min at 500 °C using trimethylgallium (TMGa) and trimethylantimony (TMSb) with molar fractions of $X_{TMGa} = 7.0 \times 10^{-5}$ and $X_{TMSb} = 8.2 \times 10^{-5}$, respectively. A resulting nanowire is depicted in Figure 1(a). Doping of the NWs is performed *in-situ* by adding the controlled amount of diethylzinc (DEZn) during the growth.

The ratio between the doping precursor and the group-III precursor (Ga) flow is used as qualitative measure of the doping level, where Zn was introduced at fractional molar flow of DEZn/TMGa = 0.006, 0.03, and 0.06. The NWs were then transferred onto a patterned Si chip ($\rho = 0.01$ Ω-cm) with 100 nm of thermally grown SiO_2. Source and drain contacts were defined on lateral NWs using electron beam lithography and lift-off with a metal evaporation of 2 nm Pd/10 nm Zn/20 nm Pd/100 nm Au. Prior to evaporation, the contact areas were ashed in oxygen plasma and wet-etched for 8 s in HCl:H_2O (1:10). To enable evaluation of the contact resistance, some NWs were processed in a four-terminal configuration. All the Si/SiO_2 device chips have an evaporated Ti (30 nm)/Au (120 nm) contact on the backside to enable the use of the highly doped Si substrate as the back gate. In order to fabricate top-gated devices, a window for high-κ dielectric was defined by EBL, followed by

a)Aein.Shiri_Babadi@EIT.LTH.SE

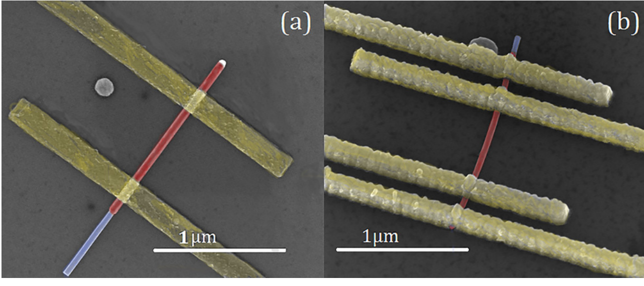

FIG. 1. False colored SEM images of a representative (a) back-gated nanowire field-effect transistor and (b) a four probe back-gated device used for the electrical transport measurements.

atomic layer deposition (ALD) and lift-off of 5 cycles of trimethylaluminum (TMA), 4 cycles of Al_2O_3 and 40 cycles of HfO_2 at 100 °C. Finally, the gate electrode was formed using EBL, evaporation, and lift-off of 30 nm Ni and 50 nm Au. The gate was designed to fully overlap both the source and drain contacts. This defines the complete active device area with a high-κ film and a top gate metal and eliminates the parasitic resistances due to ungated NW segments. All EBL patterning steps were performed using a single layer PMMA (poly-methyl methacrylate). Figure 1 depicts the SEM images of the contacted lateral single NW devices.

Electrical measurements were carried out at room temperature in ambient atmosphere, under dark conditions. The electrical properties of the GaSb NWs were first characterized using the four-point measurements to evaluate the conductivity and the contact resistance. The measured resistivity, ρ, for GaSb NWs grown with different DEZn flow is shown in Figure 2(a). The not intentionally doped GaSb NWs studied as reference showed a p-type resistivity of 0.44–1.8 Ω-cm, while the resistivity was reduced to 0.008 Ω-cm by increasing the DEZn/TMGa ratio to 0.06. The values for the nanowire resistivity were obtained by approximating the nanowires with a cylindrical geometry, $\rho = R\pi D_{NW}{}^2/4L$, where R is the measured nanowire resistance for an NW with a diameter of D_{NW} and channel length L (Table I). The contact resistance was obtained to be 0.2–0.4 kΩ (0.03–0.06 Ω·mm, normalized to the nanowire circumference) for high-doped (DEZn/TMGa = 0.06) and 15–28 kΩ (2–4 Ω·mm) for low-doped (DEZn/TMGa = 0.006) doped NWs.

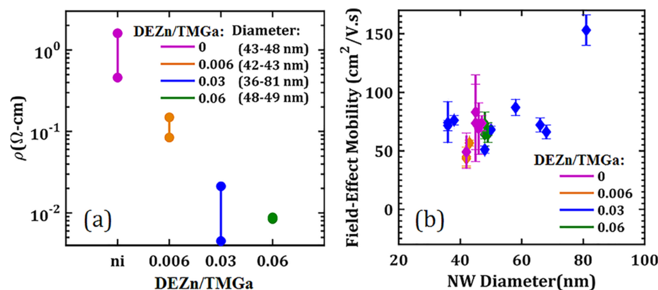

FIG. 2. (a) Measured resistivity of GaSb nanowires *versus* doping levels (DEZn/TMGa ratios). The lines illustrate the variation of resistivity measured for several devices with the same DEZn/TMGa ratio. (b) Extracted mobility as a function of nanowire diameter for various doping levels (DEZn/TMGa ratio). The lines depict the upper and lower limit of mobility obtained from V_{GS} sweeps between −10 V and 10 V in the two sweep directions.

TABLE I. Summary of the transport properties of GaSb nanowires with different doping levels. The data is presented for individual nanowire devices with long channel length $L = 550$–700 nm.

DEZn/TMGa	D_{NW}(nm)	ρ_{GaSb}(cm)	μ_h(cm^2/Vs)	p(cm^{-3})
0	47	1.8	74	4.6×10^{16}
0.006	42	0.084	57	1.3×10^{18}
0.03	50	0.012	71	7.0×10^{18}
0.06	48	0.0086	67	1.08×10^{19}

The transport properties were further evaluated by estimating the hole carrier field-effect mobilities for devices in a long channel ($L = 0.4$–1 μm) back-gated configuration. The mobility in the low field region can be calculated by $\mu_h = \frac{dI_{DS}}{dV_{GS}} \times \frac{L}{V_{DS}C_g}$, where C_g is the gate capacitance per unit length and $V_{DS} = 50$ mV. The gate capacitance C_g is determined by the series combination of oxide capacitance, C_{ox}, and the nanowire capacitance, C_q. In the diameter range of this study, C_q is expected to be sufficiently large so that $C_g \cong C_{ox}$. Here, C_{ox} is the coupling capacitance between the GaSb NW channel and the back gate through the 100-nm-thick SiO_2 gate dielectric, which is determined using the results from a finite element model (Comsol Multiphysics). The obtained mobility values are plotted versus nanowire diameters for different doping concentrations in Figure 2(b). A hysteresis exists in the transfer characteristics, which sets an upper and a lower limit to the obtained mobility reported as average value for the two gate voltage sweep directions. It is worth mentioning that the contribution of the surface/interface states capacitance, C_{it}, reduces the effective gate capacitance to $C_g{}^{eff} = C_{ox}(C_q + C_{it})/(C_{ox} + C_q + C_{it})$, which consequently indicates that the mobilities reported here from the field-effect transistors should be considered as a lower limit. The mobilities does not show any correlation with the nanowire doping [Figure 2(b)], suggesting that ionized impurity scattering is not the main limiting factor to the mobility.

To investigate how the carrier density and resistivity depend on the size of a nanowire device, the resistivity was measured for GaSb nanowires having a diameter ranging from 36 nm to 81 nm grown with DEZn/TMGa = 0.03. Figure 3(a) shows that the resistivity increases as the nanowire diameter decreases for the specific dopant concentration. In addition, a diameter-independent mobility was obtained for these GaSb nanowires, as plotted in Figure 3(b). Since the mobility is essentially independent of the diameter, the change in the resistivity has to be due to a change in hole density, p, since $p = 1/q\rho\mu_h$. The extracted hole density decreases drastically for $D_{NW} < 50$ nm [Figure 3(c)], which could be attributed to a stronger influence of a surface depletion layer formed due to interface state/trapped charges[16–18] or presence of a thin intrinsic, or even n-type, shell formed due to oxygen absorption on GaSb.[19]

The radius of the conductive core (r_C) in the NWs, assuming a surface Fermi level pinning, can be obtained from the full depletion approximation. From the Gauss law, the surface potential, $\psi(r_{NW})$, is obtained as

$$\psi(r_{NW}) = \frac{qN_a}{2\varepsilon_0\varepsilon_s}\left[r_c^2 ln\frac{r_c}{r_{NW}} + \frac{1}{2}\left(r_{NW}^2 - r_c^2\right)\right], \qquad (1)$$

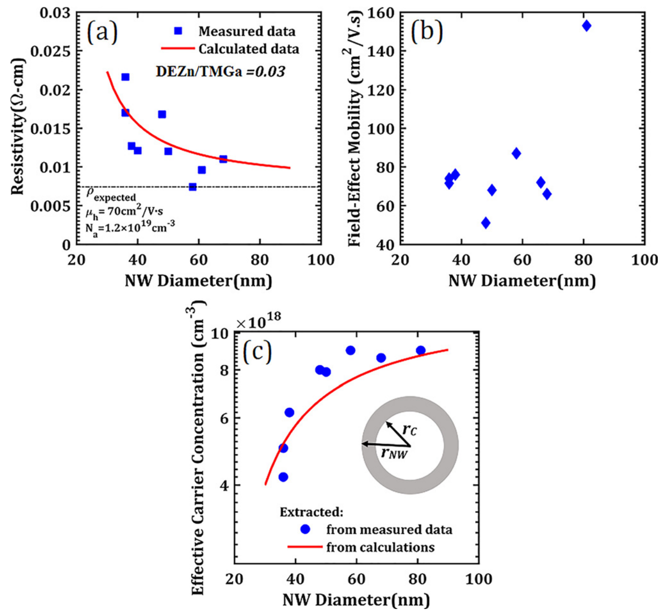

FIG. 3. Characterization of GaSb nanowires grown with DEZn/TMGa $=0.03$. (a) Extracted resistivity values from four-point measurements as a function of nanowire diameter in comparison with calculated resistivity for $N_a = 1.2 \times 10^{19}\,\mathrm{cm}^{-3}$ and $\mu_h = 70\,\mathrm{cm}^2/\mathrm{V{\cdot}s}$ (b) Calculated mobility as a function of nanowire diameter. (c) Evaluated effective carrier concentration as a function of nanowire diameter.

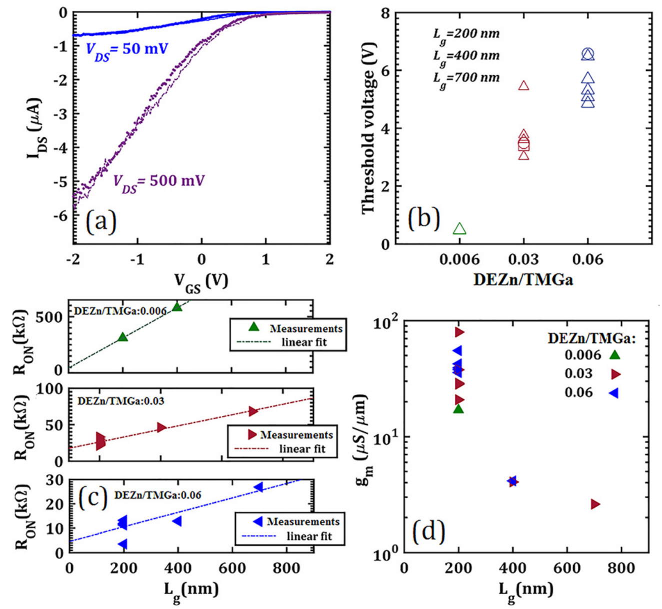

FIG. 4. (a) Transfer characteristics of a GaSb NW device with DEZn/TMGa $=0.006$ at $V_{DS} = 50\,\mathrm{mV}$ and $V_{DS} = 500\,\mathrm{mV}$, (b) V_T, (c) ON-resistance and (d) the normalized maximum transconductance as a function of gate length, L_g, for device with various doping.

where N_a is the doping concentration. Assuming a Fermi level pinning about $\varphi = 0.24\,\mathrm{eV}$ above the top of the valence band, which is in line with the findings in Ref. 20, r_C is extracted from $q\psi = 0.24 + (E_V - E_f)$. Assuming a constant mobility $\mu_h = 70\,\mathrm{cm}^2/\mathrm{V{\cdot}s}$ from the field effect mobility measurements in Figure 3(b) and a doping level $N_a = 1.2 \times 10^{19}\,\mathrm{cm}^{-3}$, the measured resistivity and effective carrier concentration can be well reproduced, as shown in Figures 3(a) and 3(c). N_a is chosen so that it represents an average carrier concentration for many devices. The estimated depletion width, $r_{NW} - r_C$, is about 6 nm for the nanowire diameters considered here.

GaSb NW MOSFETs in top-gated configuration were also characterized for NWs grown with various DEZn/TMGa ratios and diameter range of 40 nm–50 nm. The drain current as a function of gate voltage at fixed $V_{DS} = 50\,\mathrm{mV}$ and 500 mV, obtained for the NW FETs with low doping (DEZn/TMGa $= 0.006$), is shown in Figure 4(a). A linear extrapolation of threshold voltage for this device gives $V_T = 0.47\,\mathrm{V}$ that becomes more positive for NW devices grown with higher DEZn/TMGa ratio, as expected [Figure 4(b)]. For the investigated channel lengths ($L = 200$, 400, and 700 nm), a linear dependence of the device ON-resistances as a function of channel length is observed [Figure 4(c)]. The contact resistance was determined from linear extrapolation to be 0.35 Ω·mm (2.3 kΩ) and 3.1 Ω·mm (21 kΩ) to high-doped (DEZn/TMGa $= 0.06$) and low-doped (DEZn/TMGa $= 0.006$) doped NWs, respectively, which is consistent with the contact resistances obtained from four-point measurements. The normalized maximum transconductance is plotted as a function of channel length for different doping and gate lengths in Figure 4(d). A higher transconductance was achieved by scaling down the channel length reaching a maximum value of $80\,\mu\mathrm{S}/\mu\mathrm{m}$ at 200 nm L. The normalized drain current as a function of drain voltage for different gate voltages is plotted in Figures 5(b)–5(d). The *I–V* characteristics are presented for the devices with channel length, $L = 200\,\mathrm{nm}$. A too high doping combined with too large nanowire diameter does not allow for channel pinch off for DEZn/TMGa > 0.03. A larger gate modulation is obtained for the NW devices grown with the lowest DEZn flow (DEZn/TMGa $= 0.006$). However, the device shows a lower peak g_m and I_{ON}, which is attributed to a larger depletion depth[18,21] and an increase in contact resistances.

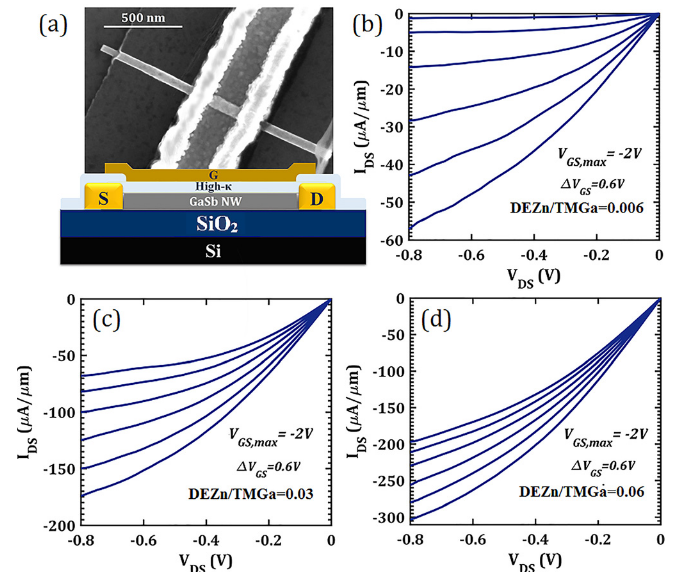

FIG. 5. (a) Schematic and SEM image of the top-gated GaSb FETs. Device output characteristics normalized for NWs circumference for various GaSb doping level with DEZn/TMGa ratio of (b) 0.006, (c) 0.03, and (d) 0.06. *I-V* characterization measured at room temperature for the top-gated GaSb FETs with channel length, $L = 200\,\mathrm{nm}$. V_{GS} is changed in steps of 0.6 V from $V_{GS} = -2\,\mathrm{V}$ up to $V_{GS} = 2\,\mathrm{V}$. The lowest subthreshold swing was measured to be 820 mV/dec for GaSb nanowire with DEZn/TMGa $= 0.03$. The NW diameter for each device was directly obtained from SEM analysis.

To summarize, we have investigated the effects of various doping profiles on the transport properties of GaSb nanowires. Our measurements show that increasing the doping during the growth of GaSb NWs increased the conductivity. The average room temperature field-effect mobility from long channel back-gated devices is 85 cm^2/V·s for unintentionally doped nanowires with $D_{NW} = 45$ nm. A peak mobility of 153 cm^2/V·s was measured for a medium doped nanowire with a larger diameter of $D_{NW} = 81$ nm. In addition, mobility is shown to be independent of nanowire diameter for the diameters in the range of 36 nm–68 nm. A high transconductance was achieved by scaling down the channel length reaching a maximum value of 80 μS/μm at 200 nm L for a top-gated GaSb nanowire transistor. The lowest contact resistance obtained was 0.35 Ω·mm for transistors with the highest doping concentration. In conclusion, our results highlight the importance of nanowire geometry and doping that are crucial for the further optimization of GaSb p-MOSFETs.

This work was supported in part by the Swedish Foundation for Strategic Research (SSF) and in part by the European Union (EU) through the H2020 Program INSIGHT under Grant Agreement No. 688784. The authors would like to thank Claes Thelander for providing the LabView program used to design the devices.

[1]H. Riel, L.-E. Wernersson, M. Hong, and J. A. del Alamo, MRS Bull. **39**(08), 668–677 (2014).
[2]J. Svensson, A. W. Dey, D. Jacobsson, and L.-E. Wernersson, Nano Lett. **15**(12), 7898–7904 (2015).
[3]K. Tomioka and T. Fukui, J. Phys. D: Appl. Phys. **47**(39), 394001 (2014).
[4]F. Glas, Phys. Rev. B **74**(12), 121302 (2006).
[5]B. M. Borg and W. Lars-Erik, Nanotechnology **24**(20), 202001 (2013).
[6]M. Jeppsson, K. A. Dick, H. A. Nilsson, N. Sköld, J. B. Wagner, P. Caroff, and L.-E. Wernersson, J. Cryst. Growth **310**(23), 5119–5122 (2008).
[7]Z.-X. Yang, F. Wang, N. Han, H. Lin, H.-Y. Cheung, M. Fang, S. Yip, T. Hung, C.-Y. Wong, and J. C. Ho, ACS Appl. Mater. Interfaces **5**(21), 10946–10952 (2013).
[8]Z.-X. Yang, N. Han, M. Fang, H. Lin, H.-Y. Cheung, S. Yip, E.-J. Wang, T. Hung, C.-Y. Wong, and J. C. Ho, Nat. Commun. **5**, 5249 (2014).
[9]X. Weng, R. A. Burke, E. C. Dickey, and J. M. Redwing, J. Cryst. Growth **312**(4), 514–519 (2010).
[10]A. W. Dey, J. Svensson, B. M. Borg, M. Ek, and L.-E. Wernersson, Nano Lett. **12**(11), 5593–5597 (2012).
[11]A. C. Ford, J. C. Ho, Y.-L. Chueh, Y.-C. Tseng, Z. Fan, J. Guo, J. Bokor, and A. Javey, Nano Lett. **9**(1), 360–365 (2009).
[12]Z.-X. Yang, S. Yip, D. Li, N. Han, G. Dong, X. Liang, L. Shu, T. F. Hung, X. Mo, and J. C. Ho, ACS Nano **9**(9), 9268–9275 (2015).
[13]M. Scheffler, S. Nadj-Perge, L. P. Kouwenhoven, M. T. Borgström, and E. P. A. M. Bakkers, J. Appl. Phys. **106**(12), 124303 (2009).
[14]B. M. Borg, M. Ek, B. Ganjipour, A. W. Dey, K. A. Dick, L.-E. Wernersson, and C. Thelander, Appl. Phys. Lett. **101**(4), 043508 (2012).
[15]G. Sepideh, J. Sofia, B. M. Borg, L. Erik, A. D. Kimberly, and W. Lars-Erik, Nanotechnology **23**(1), 015302 (2012).
[16]M. T. Bjork, H. Schmid, J. Knoch, H. Riel, and W. Riess, Nat. Nanotechnol. **4**(2), 103–107 (2009).
[17]V. Schmidt, S. Senz, and U. Gösele, Appl. Phys. A **86**(2), 187–191 (2006).
[18]B. S. Simpkins, M. A. Mastro, C. R. Eddy, and P. E. Pehrsson, J. Appl. Phys. **103**(10), 104313 (2008).
[19]W. Xu, A. Chin, L. Ye, C. Z. Ning, and H. Yu, J. Appl. Phys. **111**(10), 104515 (2012).
[20]R. Kudrawiec, H. P. Nair, M. Latkowska, J. Misiewicz, S. R. Bank, and W. Walukiewicz, J. Appl. Phys. **112**(12), 123513 (2012).
[21]V. V. Dobrokhotov, D. N. McIlroy, M. G. Norton, and C. A. Berven, Nanotechnology **17**(16), 4135 (2006).